Materials and Coatings Fabricated Using the Additive Manufacturing Technologies
Материалы и покрытия, получаемые методами аддитивных технологий

UDC 621.762

https://doi.org/10.17073/1997-308X-2024-1-52-61

Research article
Научная статья

Mechanical properties of the VZh159–CuCr1Zr alloy multi-material samples manufactured by selective laser melting

A. V. Repnin, **E. V. Borisov**, **A. A. Popovich**, **N. A. Golubkov**

Peter the Great St. Petersburg Polytechnic University
29 Polytekhnicheskaya Str., St. Petersburg 195251, Russian Federation

repnin_arseniy@mail.ru

Abstract. Selective laser melting (SLM) proves to be a suitable method for fabricating multi-material products, offering heightened performance. The objective of this study is to examine the mechanical properties of the VZh159–CuCr1Zr multi-material system produced through selective laser melting. We conducted tensile and compressive strength tests on these samples, followed by fractography, examination of polished sections, and a comparison of measured mechanical properties with existing data. Our findings are summarized as follows: the phase compositions in the regions of pure alloy denote solid solutions. *X*-ray diffraction (XRD) patterns of the interface zone reveal peaks corresponding to both alloys. The tensile strength of VZh159–CuCr1Zr multi-material samples, as measured in tensile tests, is $\sigma_u = 430 \pm 20$ MPa, with a relative elongation of $\varepsilon = 4.6 \pm 0.3$ %. Results from compressive strength tests show values of $\sigma_u = 822 \pm 23$ MPa, and relative compression $\varepsilon = 42.5 \pm 1.5$ %. Comparing these values with those of the pure CuCr1Zr alloy, the ultimate tensile strength is approximately 53 % higher (according to available data), while the conditional yield strength is about 80 % higher. Fractography of the VZh159–CuCr1Zr multi-material sample after tensile tests indicates that the interface zone exhibits both more ductile fracture features characteristic of the CuCr1Zr alloy (pits and a lack of a smooth surface) and less ductile features characteristic of the VZh159 alloy (microcracks). Examination of the polished section of a VZh159–CuCr1Zr multi-material sample after compressive strength tests reveals that the presence of a more ductile CuCr1Zr alloy in the interface zone contributes to arresting the crack, which propagates at a 45° angle to the direction of load application in the VZh159 alloy region.

Keywords: selective laser melting, multi-materials, mechanical properties, fractography, crack propagation, VZh159–CuCr1Zr

Acknowledgements: This study received support from Grant No. 23-79-30004 from the Russian Science Foundation, https://rscf.ru/project/23-79-30004/.

For citation: Repnin A.V., Borisov E.V., Popovich A.A., Golubkov N.A. Mechanical properties of the VZh159–CuCr1Zr alloy multi-material samples manufactured by selective laser melting. *Powder Metallurgy and Functional Coatings*. 2024;18(1):52–61. https://doi.org/10.17073/1997-308X-2024-1-52-61

Исследование механических свойств мультиматериальных образцов системы ВЖ159–БрХЦрТ, полученных методом селективного лазерного плавления

А. В. Репнин, Е. В. Борисов, А. А. Попович, Н. А. Голубков

Санкт-Петербургский политехнический университет Петра Великого
Россия, 195251, г. Санкт-Петербург, ул. Политехническая, 29

repnin_arseniy@mail.ru

Аннотация. Используя метод селективного лазерного плавления, можно успешно получать мультиматериальные изделия. Такие изделия будут обладать повышенными эксплуатационными характеристиками. Цель данной работы – изучение механических свойств мультиматериальной системы ВЖ159–БрХЦрТ В, полученной методом селективного лазерного плавления. Были проведены испытания ее образцов на растяжение и сжатие, после чего осуществлена их фрактография, исследованы шлифы после сжатия, выполнено сравнение полученных механических свойств с литературными данными. В результате сделаны следующие выводы: в зонах чистых сплавов фазовый состав представляет собой соответствующие твердые растворы, в переходной зоне наблюдаются пики, расположение которых соответствует пикам из обоих сплавов. При испытаниях на растяжение предел прочности мультиматериальных образцов системы ВЖ159–БрХЦрТ В составил $\sigma_в = 430 \pm 20$ МПа, относительное удлинение $\varepsilon = 4{,}6 \pm 0{,}3$ %, результаты на сжатие – $\sigma_в = 822 \pm 23$ МПа, относительное сжатие $\varepsilon = 42{,}5 \pm 1{,}5$ %. По сравнению с чистым сплавом БрХЦрТ В предел прочности мультиматериальных образцов системы ВЖ159–БрХЦрТ при испытаниях на растяжение выше на ~53 % (при сопоставлении с литературными данными), условный предел текучести в экспериментах на сжатие – на ~80 %. Фрактография мультиматериального образца системы ВЖ159–БрХЦрТ В после проведения испытаний на растяжение свидетельствует о том, что переходной зоне присущи признаки как более вязкого разрушения, характерного для сплава БрХЦрТ В (наличие ямок и отсутствие гладкого рельефа), так и менее вязкого, характерного для сплава ВЖ159 (наличие микротрещин). Исследование шлифа мультиматериального образца системы ВЖ159–БрХЦрТ В после испытаний на сжатие показало, что наличие в переходной зоне более вязкого сплава БрХЦрТ В способствует остановке развития трещины.

Ключевые слова: селективное лазерное плавление, мультиматериалы, механические свойства, фрактография, распространение трещины, ВЖ159–БрХЦрТ В

Благодарности: Исследование выполнено за счет гранта Российского научного фонда № 23-79-30004, https://rscf.ru/project/23-79-30004/.

Для цитирования: Репнин А.В., Борисов Е.В., Попович А.А., Голубков Н.А. Исследование механических свойств мультиматериальных образцов системы ВЖ159–БрХЦрТ, полученных методом селективного лазерного плавления. *Известия вузов. Порошковая металлургия и функциональные покрытия*. 2024;18(1):53–61. https://doi.org/10.17073/1997-308X-2024-1-52-61

Introduction

Additive manufacturing (AM) has become widely prevalent in high-tech industries such as petrochemicals, manufacturing, and power generation, among others [1]. One contributing factor is that AM processes can yield geometrically-complex products at a lower manufacturing cost compared to conventional methods [2]. To fabricate products from metals and alloys, diverse At can be employed. These include extrusion and deposition, laminated object manufacturing, binder jetting, direct deposition, and template-assisted synthesis. The latter involves building parts from 3D models by fusing thin layers of metal powder with an energy source [3–5].

Selective Laser Melting (SLM) is particularly notable for its ability to produce parts with variable chemical composition and enhanced performance [6]. Such products can be categorized into two groups: Functionally Graded Materials (FGM) and multi-materials [7]. Chen K. et al. [8] conducted a study on the 316L/CuSn10 multi-material system (316L being an austenitic stainless steel, and CuSn10 a tin bronze) using the SLM process. They successfully manufactured compact samples devoid of macrocracks in the interface zone. Their findings revealed a gradual decrease in Vickers microhardness from 330 HV in the 316L region to 173 HV in the CuSn10 region. The tensile and flexural strengths of the 316L/CuSn10 multi-material samples fell within the strength values for 316L and CuSn10, respectively. The shear stress of the 316L/CuSn10 sample measured 210 MPa, surpassing that of the same alloy manufactured by alternative processes.

Chen J. et al. [9] conducted a study on the same multi-material system and process. The Vickers microhardness perpendicular to the transition ranged from 230 HV in the 316L region to 155 HV in the CuSn10 region. The ultimate strength of the 316L/CuSn10 multi-material samples was measured at 420 MPa. Fracture curves indicated brittle fracture in the interface zone. SEM analysis revealed a width of approximately 550 μm for the interface zone, containing dendritic crack sources towards the steel interface.

Mei X. et al. [10] manufactured SLM samples and studied the 316L/IN718 system, where IN718 is an Inconel 718 heat-resistant nickel alloy. These samples exhibited an ultimate strength of 600 MPa and a relative elongation of 28 %. Optical microscopy, SEM, and energy-dispersive spectroscopy studies unveiled an interface zone width of approximately 100 μm, characterized by the occurrence of cracks and defects. It was suggested that to mitigate these defects, adjustments to 3D printing conditions should be made in the transition area for 316L/IN718 alloy multi-material samples.

Yusuf S. et al. [11] conducted similar studies, successfully producing compact samples with low porosity (~0.81 % on average). Metallographic analysis revealed dense dislocation networks in the interface zone, containing NbC and TiC carbides along with a small amount of Laves phases (<2 wt. %). The interfacial region exhibited equiaxed grains (average size – 45 μm), while columnar grains (average sizes – 55 and 85 μm) were observed in the pure IN718 and 316L alloy regions, respectively. Vickers microhardness (HV) measurements indicated that the hardness of the interface zone fell between the hardness values of the pure alloy regions.

Onuike B. et al. [12] investigated the IN718/GRCop-84 system (GRCop-84 being a heat-resistant bronze alloy) using a direct laser deposition process. Two approaches to producing multi-material samples were studied: direct deposition of GRCop-84 on IN718 and compositional gradation of the two alloys. The second approach yielded samples with fewer defects, while the first approach did not produce positive results. Metallographic studies revealed that the interface contained columnar grain structures and an accumulation of Cr_2Nb intermetallides. The thermal conductivity of the IN718/GRCop-84 multi-material samples was approximately 250 % higher compared to the pure IN718 alloy.

Marques A. et al. [13] made a sample representing a combustion chamber of a rocket engine, with cooling channels made of pure copper and the body constructed from the IN718 heat-resistant nickel alloy. The areas composed of pure IN718 alloy exhibited minimal defects, while defects were observed in the copper channels, distinguishable by their distinctive 200 μm width. The interface zone width was approximately 25 μm, and no intermetallic compounds were identified.

Ringel B. et al. [14] also produced a sample, a burner nozzle, using the IN718/CuCr1Zr multi-material system (CuCr1Zr being a heat-resistant bronze alloy). The cooling channels were made of CuCr1Zr, and the housing was composed of IN718. While the sample exhibited some defects, it demonstrated good processability. The width of the interface zone varied with its inclination relative to the build direction. The multi-material product structure contributed to enhanced heat transfer. The authors underscored the necessity for multi-material fabrication equipment.

Repnin A. et al. [15] investigated the impact of 3D printing parameters on the interface zone porosity in VZh159–CuCr1Zr multi-material samples, as well as the effects of heat treatment on microstructure, chemical composition, and phase compositions. The study revealed that a substantial increase in input energy was effective in reducing interface zone porosity in multi-material samples. However, common heat treatment processes applied to CuCr1Zr and VZh159 alloys did not significantly affect the microstructure, chemical composition, and phase compositions of the interface zones. The authors estimated the size of the interface zones at 300 μm when CuCr1Zr is deposited on VZh159. Unfortunately, the study did not include mechanical testing of the samples to identify the effects of a multi-material structure on material properties.

The literature review suggests that SLM can be employed to produce low-defect multi-material products, particularly in systems such as steel-bronze, steel-heat-resistant nickel alloy, and heat-resistant nickel alloy-heat-resistant bronze. However, the latter system remains poorly studied, lacking information on its mechanical properties at both room and elevated temperatures. Thus, the objective of this study is to investigate the mechanical properties of the heat-resistant nickel alloy-heat-resistant bronze system (VZh159–CuCr1Zr) obtained through SLM. To fulfill this objective, the following tasks were undertaken: conducting tensile and compressive strength tests on the multi-material samples, performing fractography after tensile tests, analyzing polished sections post-compression, and comparing the measured mechanical properties with available data.

Materials and methods

We used an SLM 280HL 3D printer (SLM Solutions, Germany) for the fabrication of multi-

material samples comprising VZh159–CuCr1Zr alloys, which were subsequently subjected to tensile and compressive strength tests. The samples were constructed using VZh159 and CuCr1Zr spherical powders (Fig. 1, Table 1), both of which were produced through atomization. Particle size distribution for the powders was determined employing the laser diffraction method with an Analysette 22 NanoTec plus system (Fritsch GmbH, Germany). The particle size distributions for the VZh159 and CuCr1Zr alloys are as follows (μm): d_{10} = 17, d_{50} = 32, d_{90} = 55 and d_{10} = 14, d_{50} = 29, d_{90} = 52.

The VZh159–CuCr1Zr multi-material samples were produced using SLM, involving 3D printing of the CuCr1Zr alloy onto the VZh159 alloy. To minimize defects in the interface zone (12 layers), the printing settings were adjusted from the standard settings for VZh159 [16] and CuCr1Zr alloys [17]. Table 2 details the SLM settings for the VZh159–CuCr1Zr multi-material sample printing. Fig. 2 illustrates the samples post-fabrication. For the tensile tests, the sample dimensions are as follows (mm): tested area width – 5, length – 20, thickness – 2 (1 mm each of VZh159 and CuCr1Zr alloys along the entire length of the sample), width of the grips – 8.2, length of the grips – 15. The dimensions for the compressive strength tests are as follows (mm): height – 7, width – 4.5, thickness – 6 (3 mm of VZh159–CuCr1Zr alloys along the entire height of the sample). The compressive test samples made of the CuCr1Zr alloy have the following dimensions (mm): height – 8.3; width and thickness – 3.

The heat treatment conditions for the VZh159–CuCr1Zr multi-material samples adhered to the standard VZh159 heat treatment procedures [18]. The heat treatment comprised five stages:

1) heating to 800 °C (10 °C/min heating rate);

2) holding for 8 h;

3) cooling to 700 °C in the furnace;

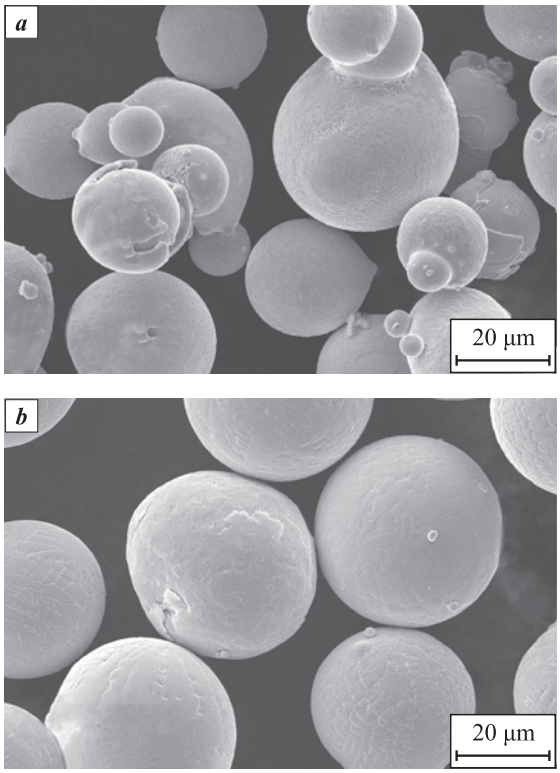

Fig. 1. Metal powder morphology
a – VZh159; ***b*** – CuCr1Zr

Рис. 1. Морфология металлического порошка
a – сплав ВЖ159, ***b*** – сплав БрХЦрТ В

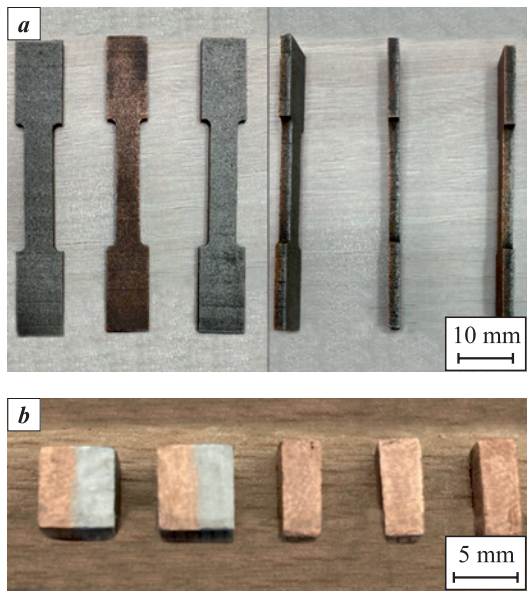

Fig. 2. VZh159–CuCr1Zr multi-material samples after SLM fabrication and machining
a – tensile test samples, ***b*** – compressive strength samples

Рис. 2. Мультиматериальные образцы системы ВЖ159–БрХЦрТ В после изготовления методом СЛП и механической обработки
a – образцы на растяжение, ***b*** – образцы на сжатие

Table 1. **Chemical composition, %, of VZh159 and CuCr1Zr powders**

Таблица 1. **Химический состав, %, порошков ВЖ159 и БрХЦрТ В**

Alloy	Cr	Ni	Al	Mo	Nb	Cu	Zr
VZh159	26–28	Base metal	1.25–1.55	7.0–7.8	2.7–3.4	–	–
CuCr1Zr	0.4–1.0	Up to 0.03	–	–	–	Base metal	0.03–0.08

Table 2. **SLM parameters for the manufacturing of VZh159–CuCr1Zr multi-material samples**

Таблица 2. **Параметры СЛП-процесса изготовления мультиматериальных образцов системы ВЖ159–БрХЦрТ В**

Alloy	Scanning speed, mm/s	Laser power, W	Hatch spacing, μm	Layer thickness, μm	Energy density, J/mm^3
VZh159	760	275	100	50	72
VZh159 + CuCr1Zr (12 layers)	160	400	150	50	325
CuCr1Zr	300	400	150	50	177

4) holding for 10 h;

5) air cooling.

It's noteworthy that conducting heat treatment to enhance the properties of both alloys is challenging due to the disparities in their structural and phase compositions. In the VZh159–CuCr1Zr system, the VZh159 alloy exhibits higher strength. Consequently, applying heat treatment to this alloy is more suitable. The standard heat treatment conditions for the VZh159 alloy do not alter the properties of the CuCr1Zr alloy or the interface zone between the alloys.

For mechanical testing, Zwick/Roell uniaxial floor-standing testing machines (Zwick Roell Group, Germany) were employed. Tensile tests were conducted on a Z050 machine (Zwick/Roell) at a 0.3 mm/min tensile rate, while compressive strength tests were performed on a Z100 machine (Zwick/Roell) at a 0.25 mm/min compression rate. Fractographic studies of the samples were carried out using a Mira 3 scanning electron microscope (Tescan, Czech Republic). The polished section with a crack that occurred after the compressive strength test was examined using a Leica DMi8 M optical microscope (Leica Microsystems, Germany). For phase composition analysis, a Rigaku SmartLab *X*-ray diffractometer (Rigaku Corporation, Japan) with a 100 μm pinhole was employed.

Results and discussion

Fig. 3 displays the *X*-ray diffraction patterns of the VZh159–CuCr1Zr multi-material sample in the pure alloy zones and the interface zone. The phase compositions in the pure alloy zones are characterized by solid solutions. In the XRDs of the interface zone, peaks are evident, indicating the presence of both alloys. The *X*-ray beam size was approximately 150 μm, fitting entirely within the interface zone (with a size of approximately 300 μm). The peaks in the interface zone overlap and cannot be distinctly separated, a phenomenon consistent with findings in other studies [12]. The XRD analysis did not reveal the presence of any additional phases.

Fig. 4 presents the results of tensile and compressive strength tests conducted on the VZh159–CuCr1Zr multi-material samples, along with pure CuCr1Zr alloy compressive strength tests. Table 3 provides a comparison of these test results with available data. The tensile strength of the VZh159–CuCr1Zr multi-material samples was $\sigma_u = 430 \pm 20$ MPa, and the relative elongation was $\varepsilon = 4.6 \pm 0.3$ % (see Table 3). The compressive test results were as follows: $\sigma_u = 822 \pm 23$ MPa, relative compression $\varepsilon = 42.5 \pm 1.5$ %.

Comparing the tensile test results with available data (Table 3) reveals an increase in ultimate strength by approximately 53 % relative to the pure CuCr1Zr alloy and a decrease by approximately 65 % relative to the pure VZh159 alloy. However, direct comparisons may lack precision due to variations in sample shapes and sizes among different researchers. Additionally, stress analysis considers the total cross-section containing both alloys, each comprising 50 % of the samples. Reassessing stress for the alloy with a greater impact on strength, the resulting tensile strength doubles to 860 MPa, reducing the relative difference to the pure VZh159 alloy to approximately 29 %. It's essential to note that available data [19] pertain to samples sub-

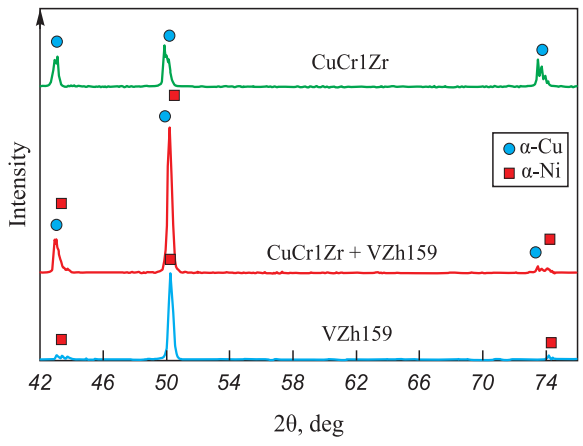

Fig. 3. Phase composition of the VZh159–CuCr1Zr multi-material samples

Рис. 3. Фазовый состав мультиматериальных образцов системы ВЖ159–БрХЦрТ В

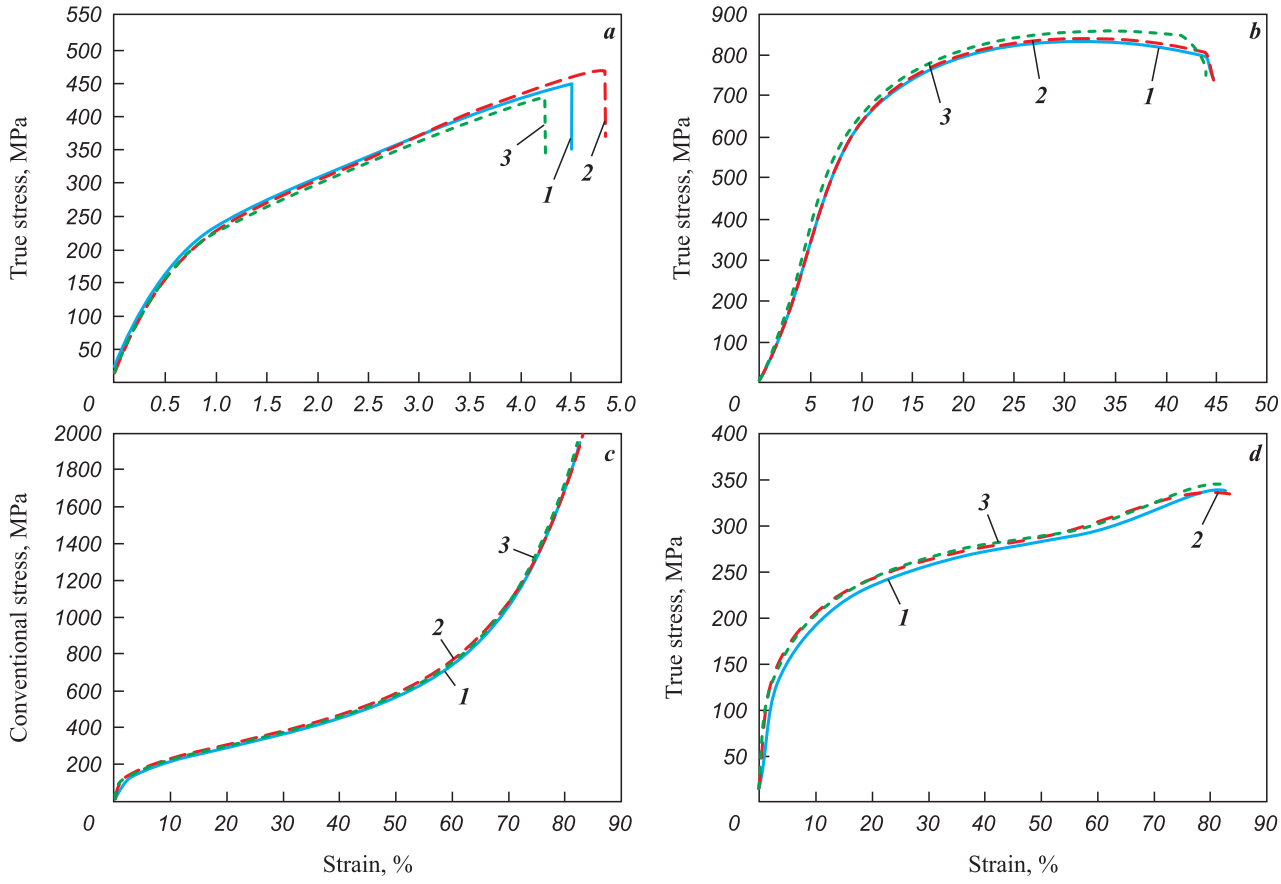

Fig. 4. Tensile (***a***) and compressive (***b***) stress-strain diagrams of the VZh159–CuCr1Zr system multi-material samples
Compressive stress-strain diagram of the pure CuCr1Zr alloy (***c*** and ***d***)

Рис. 4. Диаграмма деформирования при испытаниях на растяжение (***a***) и сжатие (***b***) мультиматериальных образцов системы ВЖ159–БрХЦрТ В, а также на сжатие чистого сплава БрХЦрТ В (***c*** и ***d***)

jected to hot isostatic pressing (HIP), a process enhancing mechanical properties, which was not conducted in this study.

The relative elongation of the VZh159–CuCr1Zr multi-material samples in the tensile tests, when compared to the pure CuCr1Zr and VZh159 alloys, reduces by 66 % and 83 %, respectively (see Table 3). This notable decrease can be attributed to the halving of the volume of the VZh159 alloy, which has a more pronounced effect on strength. Consequently, the size and number of defects in this alloy exert a greater influence on the reduction of its mechanical properties.

Comparing the results of the compressive strength test for the VZh159–CuCr1Zr multi-material samples with the available data (see Table 3) indicates a decrease in tensile strength by approximately 57 % (or 55 %) and a reduction in relative compression by 9 % (or 22 %) compared to Inconel 718 (analogous to VZh159). Similar to the analysis of tensile strength, it's important to note that stress analysis considered the entire

Table 3. **Comparison of mechanical testing results of the VZh159–CuCr1Zr multi-material samples with available data**

Таблица 3. **Сравнение результатов проведения механических испытаний мультиматериальных образцов системы ВЖ159–БрХЦрТ В с литературными данными**

Test	VZh159–CuCr1Zr multi-material samples (this study)		Alloy CuCr1Zr		Alloy VZh159		Inconel 718 alloy tests			
			[17]		[19]		[20]		[21]	
	σ_u, MPa	ε, %	σ_u, MPa	ε, %	σ_u, MPa	ε, %	σ_u, MPa	ε, %	σ_u, MPa	ε, %
Tension	430 ± 20	4.6 ± 0.3	203 ± 8	13.5 ± 2.5	1202 ± 13	26 ± 2.5	–	–	–	–
Compression	822 ± 23	42.5 ± 1.5	–	–	–	–	1900 ± 10	47 ± 2.5	1800 ± 50	55 ± 5

cross-section containing both alloys in a 1:1 ratio. After adjusting stresses for the alloy with a greater impact on strength, the reduction in ultimate strength in the specimens is 14 % and 9 %, respectively. Smith D. et al. [20] and Ghorbanpour S.et al. [21] present data for samples after HIP.

We also compared the compressive strength of the pure CuCr1Zr alloy (see Fig. 4, *c*) with available data. Our findings indicate that the properties of our samples are not inferior to those described in other studies. The offset yield strength ($\sigma_{0.2}$ true stress) of the VZh159–CuCr1Zr multi-material samples (Fig. 4, *b*) is approximately 80 % higher than that of the pure CuCr1Zr alloy (Fig. 4, *d*). Fig. 5 illustrates the VZh159–CuCr1Zr multi-material samples after the tensile and compressive strength tests.

Fig. 6 displays a fractography results of a VZh159–CuCr1Zr multi-material sample after the tensile test. In the CuCr1Zr alloy region, pits of various sizes and pores are evident, but microcracks are not present. The VZh159 alloy region exhibits a smooth fracture surface with some microcracks, suggesting that this region is more brittle compared to the CuCr1Zr region. In the interface zone, there are pits and an absence of a smooth surface, along with some microcracks. This observation implies that the interface zone exhibits both more ductile fracture features characteristic of the CuCr1Zr alloy (pits and no smooth surface) and less ductile fracture features characteristic of the VZh159 alloy (microcracks).

Fig. 7 shows a polished section of VZh159–CuCr1Zr multi-material samples after the compressive strength tests, along with an approximate crack pattern. The crack is oriented at 45° to the direction of load application in the VZh159 region. The crack ceases in the interface zone and does not propagate into the CuCr1Zr region. This observation suggests that the presence of a more

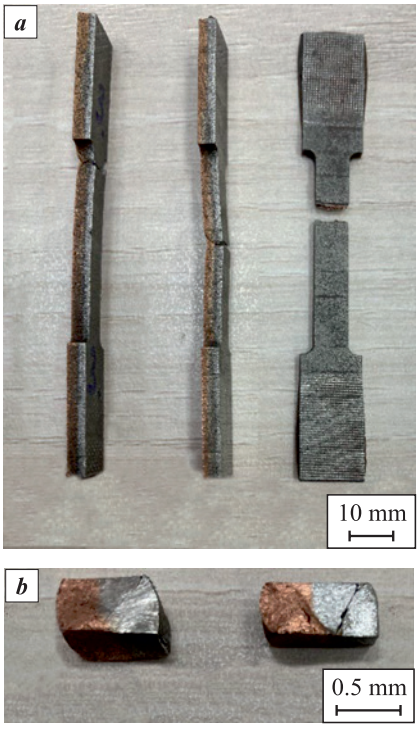

Fig. 5. VZh159–CuCr1Zr multi-material samples after tensile (***a***) and compressive strength (***b***) tests

Рис. 5. Мультиматериальные образцы системы ВЖ159–БрХЦрТ В после проведения испытаний на растяжение (***a***) и сжатие (***b***)

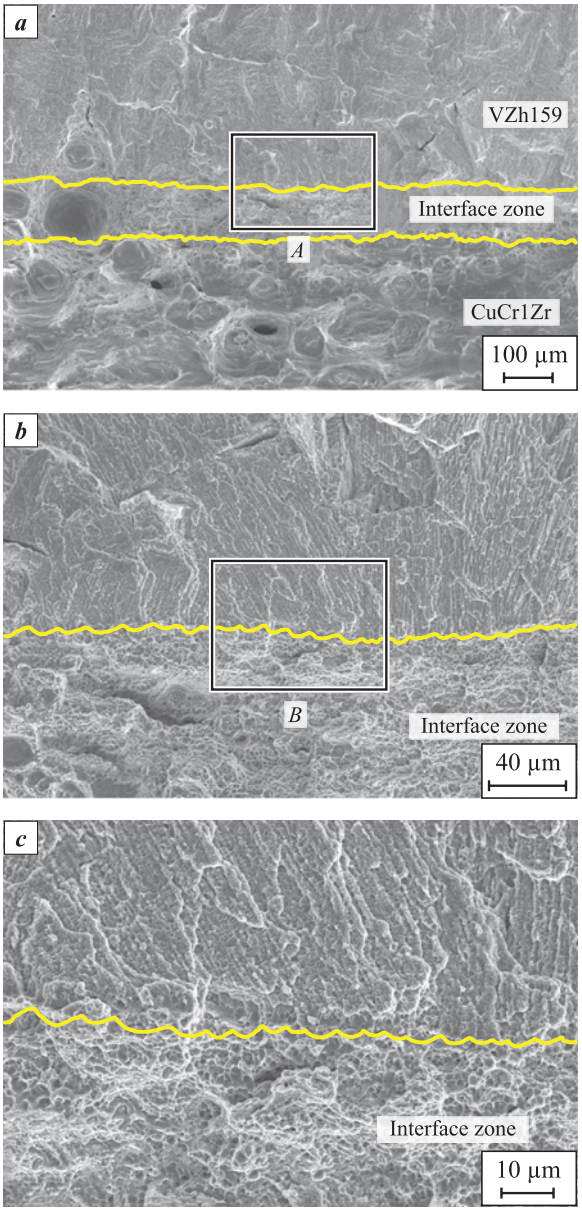

Fig. 6. Fractography of a VZh159–CuCr1Zr multi-material sample after tensile tests
a – general view, ***b*** – area *A*, ***c*** – area *B*

Рис. 6. Фрактография мультиматериального образца системы ВЖ159–БрХЦрТ В после проведения испытаний на растяжение
a – общий вид, ***b*** – область *A*, ***c*** – область *B*

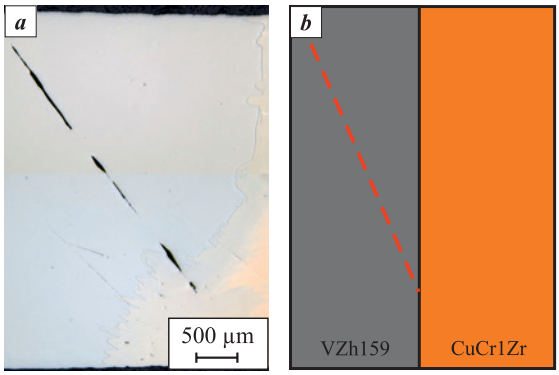

Fig. 7. Polished section of VZh159–CuCr1Zr multi-material samples after compressive strength tests (***a***) and approximate crack pattern (***b***)

Рис. 7. Шлиф мультиматериального образца системы ВЖ159–БрХЦрТ В после проведения испытаний на сжатие (***a***) и схематичное изображение распространения трещины (***b***)

ductile CuCr1Zr alloy in the interface zone contributes to the cessation of crack propagation.

Conclusions

In our investigation of the VZh159–CuCr1Zr multi-material system, we explored the phase composition of the interface zone and assessed mechanical properties, including ultimate strength, relative elongation, and relative compression through tensile and compressive strength tests. Additionally, we conducted fractography following tensile tests and analyzed crack propagation post-compressive strength tests. Our findings led to the following conclusions:

1. The phase compositions in the pure alloy zones are solid solutions. XRD patterns of the interface zone exhibit peaks corresponding to both alloys.

2. The tensile strength of the VZh159–CuCr1Zr multi-material samples, as determined by tensile tests, is $\sigma_u = 430 \pm 20$ MPa, with a relative elongation of $\varepsilon = 4.6 \pm 0.3$ %. The results of the compressive strength test were as follows: $\sigma_u = 822 \pm 23$ MPa, and relative compression $\varepsilon = 42.5 \pm 1.5$ %.

3. Tensile tests revealed that the ultimate strength of the VZh159–CuCr1Zr multi-material samples, when compared to the pure CuCr1Zr alloy, is approximately 53 % higher (according to available data), and the conditional yield strength increases by ~80 %.

4. The fractography of the VZh159–CuCr1Zr multi-material sample after tensile tests indicates that the interface zone displays both more ductile fracture features characteristic of the CuCr1Zr alloy (pits and no smooth surface) and less ductile features characteristic of the VZh159 alloy (microcracks).

5. Examination of the polished section of a VZh159–CuCr1Zr multi-material sample after compressive strength tests demonstrates that the presence of a more ductile CuCr1Zr alloy in the interface zone contributes to arresting the crack, which propagates at 45° to the direction of load application in the VZh159 alloy region.

References / Список литературы

1. Srivastava M., Rathee S., Patel V., Kumar A., Koppad P.G. A review of various materials for additive manufacturing: Recent trends and processing issues. *Journal of Materials Research and Technology*. 2022;21:2612–2641. https://doi.org/10.1016/j.jmrt.2022.10.015
2. Ngo T.D., Kashani A., Imbalzano G., Nguyen K.T.Q., Hui D. Additive manufacturing (3D printing): A review of materials, methods, applications and challenges. *Composites, Part B: Engineering*. 2018; 143:172–196. https://doi.org/10.1016/j.compositesb.2018.02.012
3. Gunasekaran J., Sevvel P., Solomon I.J. Metallic materials fabrication by selective laser melting: A review. *Materials Today: Proceedings*. 2021;37(2):252–256. https://doi.org/10.1016/j.matpr.2020.05.162
4. Negi S., Nambolan A.A., Kapil S., Joshi P.S., Karunakaran K.P., Bhargava P. Review on electron beam based additive manufacturing. *Rapid Prototyping Journal*. 2020;26(3):485–498. https://doi.org/10.1108/RPJ-07-2019-0182
5. Sefene E.M. State-of-the-art of selective laser melting process: A comprehensive review. *Journal of Manufacturing Systems*. 2022;63:250–274. https://doi.org/10.1016/j.jmsy.2022.04.002
6. Nandhakumar R., Venkatesan K. A process parameters review on selective laser melting-based additive manufacturing of single and multi-material: Microstructure, physical properties, tribological, and surface roughness. *Materials Today Communications*. 2023;35:105538. https://doi.org/10.1016/j.mtcomm.2023.105538
7. Nazir A., Gokcekaya O., Masum Billah K., Ertugrul O., Jiang J., Sun J., Hussain S. Multi-material additive manufacturing: A systematic review of design, properties, applications, challenges, and 3D printing of materials and cellular metamaterials. *Materials & Design*. 2023;226:111661. https://doi.org/10.1016/j.matdes.2023.111661
8. Chen K., Wang C., Hong Q., Wen S., Zhou Y., Yan C., Shi Y. Selective laser melting 316L/CuSn10 multi-materials: Processing optimization, interfacial characterization and mechanical property. *Journal of Materials Processing Technology*. 2020;283:116701. https://doi.org/10.1016/j.jmatprotec.2020.116701
9. Chen J., Yang Y., Song C., Zhang M., Wu S., Wang D. Interfacial microstructure and mechanical properties of 316L/CuSn10 multi-material bimetallic structure fabricated by selective laser melting. *Materials Science and Engineering: A*. 2019;752:75–85. https://doi.org/10.1016/j.msea.2019.02.097
10. Mei X., Wang X., Peng Y., Gu H., Zhong G., Yang S. Interfacial characterization and mechanical properties

of 316L stainless steel/Inconel 718 manufactured by selective laser melting. *Materials Science and Engineering: A*. 2019;758:185–91. https://doi.org/10.1016/j.msea.2019.05.011

11. Yusuf S., Mazlan N., Musa N.H., Zhao X., Chen Y., Yang S., Nordin N.A., Mazlan S.A., Gao N. Microstructures and hardening mechanisms of a 316L stainless steel/Inconel 718 interface additively manufactured by multi-material selective laser melting. *Metals*. 2023;13(2):400. https://doi.org/10.3390/met13020400
12. Onuike B., Heer B., Bandyopadhyay A. Additive manufacturing of Inconel 718 – Copper alloy bimetallic structure using laser engineered net shaping (LENSTM). *Additive Manufacturing*. 2018;21:133–140. https://doi.org/10.1016/j.addma.2018.02.007
13. Marques A., Cunha Â., Gasik M., Carvalho O., Silva F.S., Bartolomeu F. Inconel 718 – copper parts fabricated by 3D multi-material laser powder bed fusion: a novel technological and designing approach for rocket engine. *The International Journal of Advanced Manufacturing Technology*. 2022;122:2113–2123. https://doi.org/10.1007/s00170-022-10011-x
14. Ringel B., Zaepfel M., Herlan F., Horn M., Schmitt M., Seidel C. Advancing functional integration through multi-material additive manufacturing: Simulation and experimental validation of a burner nozzle. *Materials Today: Proceedings*. 2022;70:296–303. https://doi.org/10.1016/j.matpr.2022.09.241
15. Repnin A.V., Borisov E.V., Popovich A.A., Shamshurin A.I. Selective laser melting of multi-material VZh159–CuCr1Zr samples. *Global Energy*. 2023;29(2):175–188. (In Russ.). https://doi.org/10.18721/JEST.29212

    Репнин А.В.. Борисов Е.В., Попович А.А., Шамшурин А.И. Создание мульти-материальных образцов системы ВЖ159–БрХЦрТ методом селективного лазерного плавления. *Глобальная энергия*. 2023;29(2):175–188. https://doi.org/10.18721/JEST.29212
16. Popovich A.A., Sufiiarov V.S., Polozov I.A., Borisov E.V. Microstructure and mechanical properties of Inconel 718 produced by SLM and subsequent heat treatment. *Key Engineering Materials*. 2015;651–653:665–670.
17. Artemov A.L., Dyadchenko V.Yu., Lukyashko A.V., Novikov A.N., Popovich A.A., Rudskoy A.I., Svechkin V.P., Skoromnov V.I., Smolentsev A.A., Sokolov B.A., Solntsev V.L., Sufiyarov V.Sh., Shachnev S.Yu, Development of design and technology solutions for additive manufacturing of prototype inner lining for combustion chamber of multifunctional liquid-propellant rocket engine. *Space Technique and Technologies*. 2017;1(16):50–62. (In Russ.).

    Артемов А.Л., Дядченко В.Ю., Лукьяшко А.В., Новиков А.Н., Попович А.А., Рудской А.И., Свечкин В.П., Скоромнов В.И., Смоленцев А.А., Соколов Б.А., Солнцев В.Л., Суфияров В.Ш., Шачнев С.Ю. Отработка конструктивных и технологических решений для изготовления опытных образцов внутренней оболочки камеры сгорания многофункционального жидкостного ракетного двигателя с использованием аддитивных технологий. *Космическая техника и технологии*. 2017;1(16):50–62.
18. Khlybov A.A., Belyaev E.S., Ryabtsev A.D., Belyaeva S.S., Getmanovsky Y.A., Yavtushenko P.M., Ryabov D.A. Influence of the HIP technology on the structure and properties of nickel alloy VZH159. *Vestnik of Nosov Magnitogorsk State Technical University*. 2021;3:75–83. (In Russ.). https://doi.org/10.18503/1995-2732-2021-19-3-75-83

    Хлыбов А.А., Беляев Е.С., Рябцев А.Д., Беляева С.С., Гетмановский Ю.А., Явтушенко П.М., Рябов Д.А. Влияние технологии ГИП на структуру и свойства никелевого сплава ВЖ 159. *Вестник Магнитогорского государственного технического университета*. 2021;3:75–83. https://doi.org/10.18503/1995-2732-2021-19-3-75-83
19. Prager S.M., Solodova T.V., Tatarenko O.Y. Research of mechanical properties and microstructure of samples obtained by SLS from metal powder composition of VZh159 alloy. *Proceedings of VIAM*. 2017;11:1–11. (In Russ.). https://dx.doi.org/10.18577/2307-6046-2017-0-11-1-1

    Прагер С.М., Солодова Т.В., Татаренко О.Ю. Исследование механических свойств и структуры образцов, полученных методом селективного лазерного сплавления (СЛС) из сплава ВЖ159. *Труды ВИАМ*. 2017;11:1–11. https://dx.doi.org/10.18577/2307-6046-2017-0-11-1-1
20. Smith D.H., Bicknell J., Jorgensen L., Patterson B.M., Cordes N.L., Tsukrov I., Knezevic M. Microstructure and mechanical behavior of direct metal laser sintered Inconel alloy 718. *Materials Characterization*. 2016;113(1):1–9.
21. Ghorbanpour S., Alam M.E,. Ferreri N.C., Kumar A., McWilliams B.A., Vogel S.C., Bicknell J., Beyerlein I.J., Knezevic M. Experimental characterization and crystal plasticity modeling of anisotropy, tension-compression asymmetry, and texture evolution of additively manufactured Inconel 718 at room and elevated temperatures. *International Journal of Plasticity*. 2020;125:63–79. https://doi.org/10.1016/j.ijplas.2019.09.002
22. Bai Y., Zhao C., Zhang Y., Chen J., Wang H. Additively manufactured CuCrZr alloy: Microstructure, mechanical properties and machinability. *Materials Science and Engineering: A*. 2021;819:141528. https://doi.org/10.1016/j.msea.2021.141528

Information about the Authors

Arseniy V. Repnin – Engineer, Laboratory "Synthesis of new materials and structures", Peter the Great St. Petersburg Polytechnic University (SPbPU)
ORCID: 0009-0001-3157-3317
E-mail: repnin_arseniy@mail.ru

Сведения об авторах

Арсений Вячеславович Репнин – инженер лаборатории «Синтез новых материалов и конструкций» Санкт-Петербургского политехнического университета Петра Великого (СПбПУ)
ORCID: 0009-0001-3157-3317
E-mail: repnin_arseniy@mail.ru

Evgeny V. Borisov – Cand. Sci. (Eng.), Leading Researcher, Laboratory "Synthesis of new materials and structures", SPbPU
ORCID: 0000-0003-2464-6706
E-mail: evgenii.borisov@icloud.com

Anatoly A. Popovich – Dr. Sci. (Eng.), Professor, Director of the Institute of Machinery, Materials, and Transport, SPbPU
ORCID: 0000-0002-5974-6654
E-mail: popovicha@mail.ru

Nikita A. Golubkov – Lead Engineer, Laboratory "Synthesis of new materials and structures", SPbPU
ORCID: 0009-0009-6785-1444
E-mail: golubkovna@gmail.com

Евгений Владиславович Борисов – к.т.н., ведущий научный сотрудник лаборатории «Синтез новых материалов и конструкций» СПбПУ
ORCID: 0000-0003-2464-6706
E-mail: evgenii.borisov@icloud.com

Анатолий Анатольевич Попович – д.т.н., профессор, директор Института машиностроения, материалов и транспорта СПбПУ
ORCID: 0000-0002-5974-6654
E-mail: popovicha@mail.ru

Никита Александрович Голубков – ведущий инженер лаборатории «Синтез новых материалов и конструкций» СПбПУ
ORCID: 0009-0009-6785-1444
E-mail: golubkovna@gmail.com

Contribution of the Authors

A. V. Repnin – conducted experiments, processed the results, and wrote the initial draft manuscript.
E. V. Borisov – planned experiments, wrote the manuscript, and participated in discussions about the results.
A. A. Popovich – conceptualized the idea, determined the purpose of the work, and participated in discussions about the results.
N. A. Golubkov – carried out tensile and compression tests, and processed the results obtained.

Вклад авторов

А. В. Репнин – проведение экспериментов, обработка полученных результатов, написание черновика статьи.
Е. В. Борисов – планирование экспериментов, написание статьи, участие в обсуждении результатов.
А. А. Попович – концептуализация идеи, определение цели работы и ее задач, участие в обсуждении результатов.
Н. А. Голубков – проведение испытаний на растяжение и сжатие, обработка полученных результатов.

Received 27.06.2023
Revised 15.08.2023
Accepted 18.08.2023

Статья поступила 27.06.2023 г.
Доработана 15.08.2023 г.
Принята к публикации 18.08.2023 г.